



The effect of mAb and excipient cryoconcentration on long-term frozen storage stability – Part 1: Higher molecular weight species and subvisible particle formation

Oliver Bluemel^a, Moritz Anuschek^a, Jakob W. Buecheler^b, Georg Hoelzl^c, Karoline Bechtold-Peters^b, Wolfgang Friess^{a,*}

^a Pharmaceutical Technology and Biopharmaceutics, Department of Pharmacy, Ludwig-Maximilians-Universitaet Muenchen, 81377 Munich, Germany

^b Technical Research and Development, Novartis Pharma AG, 4002 Basel, Switzerland

^c Sandoz GmbH, 6336 Langkampfen, Austria

ARTICLE INFO

Keywords:

Cryoconcentration
Frozen storage
Large-scale freezing
Monoclonal antibody
Stability

ABSTRACT

Cryoconcentration upon large-scale freezing of monoclonal antibody (mAb) solutions leads to regions of different ratios of low molecular weight excipients, like buffer species or sugars, to protein. This study focused on the impact of the buffer species to mAb ratio on aggregate formation after frozen storage at $-80\text{ }^{\circ}\text{C}$, $-20\text{ }^{\circ}\text{C}$, and $-10\text{ }^{\circ}\text{C}$ after 6 weeks, 6 months, and 12 months. An optimised sample preparation was established to measure T_g' of samples with different mAb to histidine ratios via differential scanning calorimetry (DSC). After storage higher molecular weight species (HMWS) and subvisible particles (SVPs) were detected using size-exclusion chromatography (SEC) and FlowCam, respectively. For all samples, sigmoidal curves in DSC thermograms allowed to precisely determine T_g' in formulations without glass forming sugars. Storage below T_g' did not lead to mAb aggregation. Above T_g' , at $-20\text{ }^{\circ}\text{C}$ and $-10\text{ }^{\circ}\text{C}$, small changes in mAb and buffer concentration markedly impacted stability. Samples with lower mAb concentration showed increased formation of HMWS. In contrast, higher concentrated samples led to more SVPs. A shift in the mAb to histidine ratio towards mAb significantly increased overall stability. Cryoconcentration upon large-scale freezing affects mAb stability, although relative changes compared to the initial concentration are small. Storage below T_g' completely prevents mAb aggregation and particle formation.

1. Introduction

Therapeutic monoclonal antibodies (mAbs) are essential in the treatment of numerous diseases and part of a rapidly growing market (Arsiccio and Pisano, 2020; Mehta et al., 2019; Roessl et al., 2015). A common processing step to enhance chemical and physical stability and to minimise the risk of microbial growth is to freeze bulk drug substance (Padala et al., 2010; Rathore and Rajan, 2008; Rodrigues et al., 2011). Frozen storage and transportation offer flexibility during manufacturing and eliminates the risk of shaking and foaming (Padala et al., 2010; Rathore and Rajan, 2008; Rodrigues et al., 2011; Roessl et al., 2014). Besides sustainability concerns, mechanical stress, local pressure, the

formation of air bubbles, and oxidation are considerable drawbacks as recently highlighted (Authelin et al., 2020). Others, such as the destabilising effect of the cold temperature itself (Arsiccio et al., 2020), crystallisation of buffer components or cryoprotectants (Connolly et al., 2015; Kolhe et al., 2009; Singh et al., 2011), interfaces (Arsiccio and Pisano, 2020; Duarte et al., 2020), and cryoconcentration on a microscopic and macroscopic scale (Hauptmann et al., 2019; Kolhe et al., 2012; Roessl et al., 2015) are well known but still not completely understood. Thereby, freezing, which seems to be a simple and easily controllable process, becomes complex and the contribution of each stress on the overall stability nearly impossible to assess.

Often small-scale studies, typically performed in vials or tubes, are

Abbreviations: DSC, Differential scanning calorimetry; FCM, Freeze-concentrated matrix; HMWS, Higher molecular weight species; HPLC, High-performance liquid chromatography; mAb, Monoclonal antibody; PES, Polyethersulfone; SEC, Size-exclusion chromatography; SVP, Subvisible particle; T_g' , Glass transition temperature of the maximally freeze-concentrated solution.

* Corresponding author:

E-mail address: Wolfgang.Friess@cup.uni-muenchen.de (W. Friess).

<https://doi.org/10.1016/j.ijpx.2021.100108>

Received 21 December 2021; Accepted 22 December 2021

Available online 25 December 2021

2590-1567/© 2021 Published by Elsevier B.V. This is an open access article under the CC BY-NC-ND license (<http://creativecommons.org/licenses/by-nc-nd/4.0/>).

used to find the optimal formulation and ideal freezing and thawing conditions or to unveil unforeseen events (Connolly et al., 2015; Hauptmann et al., 2018; Kuelzto et al., 2008; Zhang et al., 2012). Connolly et al. highlighted the effects of formulation composition, cooling rate and storage temperature on mAb stability (Connolly et al., 2015). They found that trehalose crystallisation is a considerable event during storage above the glass transition temperature of the maximally freeze concentrated solution (T_g') at -8°C , -14°C and -20°C . Storage below T_g' at -40°C prevented crystallisation and consequently protein aggregation. These outcomes can be associated with the negligible molecular mobility below T_g' . Hauptmann et al. examined the particle formation caused by multiple freeze-thaw cycles with the focus on processing rates, mAb concentration and buffer formulation, but did not investigate the effect on storage stability (Hauptmann et al., 2018).

In a previous study, we examined cryoconcentration in a rectangular 2 L bottle after freezing of mAb in pure histidine buffer (Bluemel et al., 2020). Microscopically, ice crystals grow into unfrozen regions and exclude other formulation components. The mAb and excipients form a freeze-concentrated matrix (FCM) in between these ice crystals. Macroscopically, at the freezing front the solutes are transported away by natural convection and diffusion. This creates a heterogeneous distribution of solutes. In contrast to the previous scientific consensus that proteins and excipients freeze-concentrate to the same extent (Singh et al., 2009), recent studies show that large proteins are entrapped in the ice to a larger extent than small excipients (Kolhe et al., 2012; Müller et al., 2013). This is in accordance with our study, where significant shifts in the mAb to histidine ratio were observed (Bluemel et al., 2020). As the ion concentration respectively the mAb to low molecular weight excipient ratio in the FCM vary throughout the container, also self-interaction of the mAb and colloidal stability vary. In addition, T_g' as the temperature at which the highly viscous FCM forms a glass will differ with solution composition (Authelin et al., 2020; Connolly et al., 2015; Franks, 1998; Kasper and Friess, 2011). Ultimately, the mAb stability at different spots of large containers can vary.

To our knowledge, no study has connected the cryoconcentration associated with a change in mAb to excipient ratio after freezing in large-scale containers to long-term frozen storage. To assess the impact of this cryoconcentration and the shifted ratios of mAb and histidine, we prepared samples according to the concentrations found previously (Fig. 1). In the current study, we focused on the areas with minimum and maximum mAb and histidine concentrations. We stored these formulations small-scale at -80°C , -20°C , or -10°C for up to 12 months and analysed mAb aggregation. Storage below T_g' at -80°C completely prevented any formation of higher molecular weight species (HMWS) and subvisible particles (SVPs). Storage above T_g' at -20°C led to significant aggregation and SVP levels after 6 months and 12 months. This effect was boosted at -10°C . Long-term storage stability above T_g' was affected by ΔT between T_g' and the storage temperature, the ionic strength in the non-solidified FCM, and mAb concentration. Significant differences in mAb stability resulted in the samples reflecting the solute concentration variants as a consequence of cryoconcentration. Transferred to regions in a 2 L bottle the small-scale experiments indicate that highly concentrated areas in the centre and the top region in a 2 L bottle can be associated with significant formation of SVPs. In contrast, the diluted core in the geometrical centre is more prone to formation of soluble mAb aggregates. The samples containing minimum histidine, representative for the areas at the wall, showed the highest stability.

2. Materials and methods

2.1. Materials

An IgG1 mAb stock solution in histidine buffer at pH 5.5 was provided by Novartis AG (Basel, Switzerland). L-histidine and L-histidine monochloride monohydrate were obtained from Merck KGaA (Darmstadt, Germany).

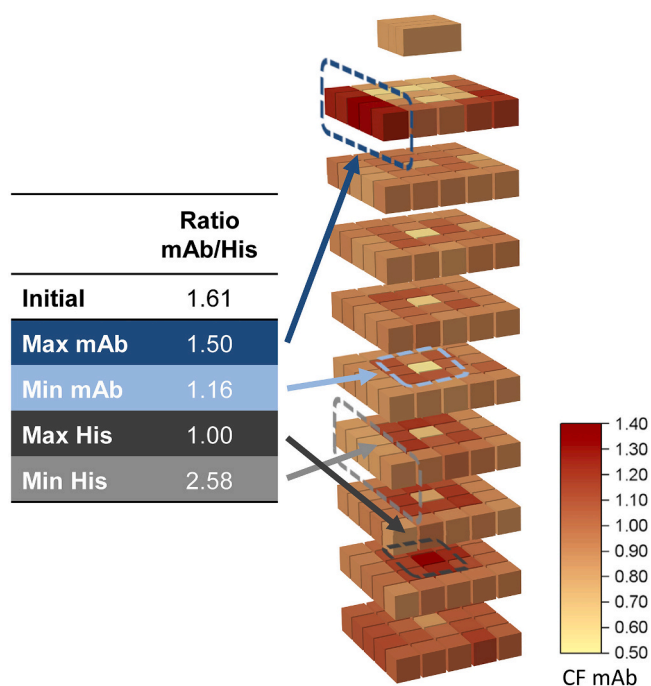


Fig. 1. Changes in mAb concentration after freezing a mAb solution in histidine in a 2 L bottle. Details were published and discussed previously (Bluemel et al., 2020). The legend highlights the cryoconcentration factor, which is the ratio of the mAb concentration of the sample to the initial mAb concentration. The mAb to histidine ratios for selected samples are given in the table. Corresponding areas are highlighted for visualisation.

Potassium dihydrogen phosphate and dipotassium hydrogen phosphate were purchased from Merck KGaA (Darmstadt, Germany).

Sucrose was obtained from Sigma-Aldrich (Steinheim am Albuch, Germany).

VWR International GmbH (Darmstadt, Germany) provided $0.2\ \mu\text{m}$ polyethersulfone (PES) membrane syringe filters. 2R glass vials were purchased from SCHOTT AG (Mainz, Germany). FluroTec® lyophilisation stoppers from West Pharmaceuticals (Eschweiler, Germany) were used.

2.2. Sample preparation

The mAb stock solution was diluted to mAb to histidine ratios given in Fig. 1. Different histidine buffers at pH 5.5 were prepared to reach the final histidine concentrations. Due to confidentiality, the exact composition of the samples may not be revealed. The mAb concentration was controlled with a NanoDrop One (Thermo Fisher Scientific Inc., Waltham, Massachusetts, USA) via UV absorption at 280 nm. Samples were filtered through $0.2\ \mu\text{m}$ PES membrane filters. Three 2R glass vials for each formulation and each time point were filled with 1 mL and semi-stoppered.

All vials were frozen in a Christ Epsilon 2-6D LSCplus (Martin Christ Gefriertrocknungsanlagen GmbH, Osterode am Harz, Germany). Samples were arranged in the centre of lyophilisation trays surrounded by two rows of vials filled with 10% (w/V) sucrose. These rows were added to minimise variations in heat transfer in the samples due to radiation, known as the edge effect during lyophilisation. Vials were cooled with 1 K/min to -5°C and this temperature held for 60 min. During this temperature plateau, controlled nucleation was induced using the Lyo-CoN ice fog technology (Martin Christ Gefriertrocknungsanlagen GmbH, Osterode am Harz, Germany). This technique introduces ice crystals for seeding of vials by aeration through the condenser. Subsequently, samples were cooled to -40°C with 1 K/min. Thereby similar ice morphology should be achieved in all samples (Bhatnagar et al., 2008;

Kasper and Friess, 2011). Afterwards, the vials were transferred to precooled $-10\text{ }^{\circ}\text{C}$ (Köttermann GmbH, Uetze, Germany), $-20\text{ }^{\circ}\text{C}$ (Liebherr, Bulle, Switzerland) and $-80\text{ }^{\circ}\text{C}$ freezers (LAUDA-GFL GmbH, Burgwedel, Germany).

2.3. Stability analysis

After 12 h of acclimatisation triplicates of each formulation were thawed at room temperature on the laboratory bench and analysed as t0. After 6 weeks, 6 months and 12 months further samples ($n = 3$) were thawed and analysed.

2.3.1. Flow imaging microscopy

SVPs were characterised with a FlowCam 8100 (Fluid Imaging Technologies, Inc., Scarborough, Maine, USA) equipped with a $10\times$ magnification cell. Particles were counted using $160\text{ }\mu\text{L}$ sample volume, a flow rate of 0.15 mL/min , an auto image frame rate of 28 frames/s and a sampling time of 60 s. Distance to the nearest neighbour for particle identification was set to $3\text{ }\mu\text{m}$. Particle segmentation thresholds of 10 for light and 13 for dark pixels were defined. Particle size was reported as the equivalent spherical diameter. The VisualSpreadsheet® 4.7.6 software was used for measuring and processing.

2.3.2. Size-exclusion chromatography

Size-exclusion chromatography (SEC) on an Agilent 1200 high-performance liquid chromatography (HPLC) system equipped with a diode array detector (Agilent Technologies, Santa Clara, California, USA) set to 220 nm was used to quantify HMWS. A TSKgel G3000 SWxl column (Tosoh Bioscience GmbH, Griesheim, Germany) as stationary phase, a 150 mM potassium phosphate buffer pH 6.5 at a flow rate of 0.4 mL/min as mobile phase, and $5\text{ }\mu\text{L}$ injection volume were used. Prior to injection all samples were centrifuged 2 min at 25.700 xg with a Heraeus™ Megafuge™ 16R (Thermo Fisher Scientific Inc., Waltham, Massachusetts, USA). Agilent OpenLAB Data Analysis Software 2.1 was used to analyse the chromatograms.

2.4. Determination of T_g'

Samples of different mAb to histidine ratios were prepared as described in 2.2. 2 mL of each solution was filled into 2R glass vials and arranged in the centre of a lyophilisation tray surrounded by vials filled with 10% (w/V) sucrose. Lyophilisation was carried out with the Christ Epsilon 2-6D LSCplus (Martin Christ Gefriertrocknungsanlagen GmbH, Osterode am Harz, Germany). Samples were frozen to $-40\text{ }^{\circ}\text{C}$ with a ramp of 1 K/min . Temperature was increased to $-20\text{ }^{\circ}\text{C}$ with 1 K/min and primary drying carried out for 35 h at a pressure of 0.09 mbar . For secondary drying a 0.3 K/min ramp to $30\text{ }^{\circ}\text{C}$ was applied and shelf temperature held for 4 h at 0.09 mbar . Afterwards, samples were stoppered at 600 mbar in a nitrogen atmosphere. Lyophilisates were reconstituted with highly purified water to 100 mg/mL mAb and after 24 h, to ensure complete dissolution, differential scanning calorimetry (DSC) measurements were carried out.

DSC thermograms were acquired with the DSC821® (METTLER TOLEDO, Columbus, Ohio, USA). Aluminium crucibles (METTLER TOLEDO, Columbus, Ohio, USA) were filled with $20\text{ }\mu\text{L}$. An empty crucible of the same type was used as reference. Samples were cooled from $25\text{ }^{\circ}\text{C}$ to $-60\text{ }^{\circ}\text{C}$ with a rate of 10 K/min . After isothermal hold for 1 min, samples were analysed while heated to $25\text{ }^{\circ}\text{C}$ at 3 K/min . T_g' was determined as the inflection point of the sigmoidal glass transition. Data analysis was carried out with the STARe-Software (METTLER TOLEDO, Columbus, Ohio, USA).

3. Results

3.1. Long-term storage at $-80\text{ }^{\circ}\text{C}$

The formation of HMWS as well as SVPs was analysed at the start and after storage for 6 weeks, 6 months, and 12 months. The results for storage at $-80\text{ }^{\circ}\text{C}$ are displayed in Fig. 2. All samples contained approximately 1.5% HMWS at the start of the experiment. This level did not increase during storage, regardless of the sample composition.

The histidine buffer control sample showed $500\text{ SVPs } \geq 1\text{ }\mu\text{m}$ per mL at the start and only a minor increase to 1900 after 12 months. All mAb containing samples displayed approximately 4000 SVPs at t0. These t0 samples had been frozen, stored at the intended temperature for 12 h, and thawed. No significant increase in SVP level could be detected during long-term storage at $-80\text{ }^{\circ}\text{C}$.

3.2. Long-term storage at $-20\text{ }^{\circ}\text{C}$

All samples stored at $-20\text{ }^{\circ}\text{C}$ again started with approximately 1.5% HMWS (Fig. 3). After 6 weeks, the soluble aggregate levels did not increase in any of the samples. In general, the increase after 6 months was still moderate, considering the following 12 months point and the changes observed after storage at $-10\text{ }^{\circ}\text{C}$ (see 3.3). After 6 months, the HMWS reached 2.2% in samples with the initial composition (mAb to histidine ratio 1.61), while samples representing maximum (ratio 1.50) and minimum mAb (ratio 1.16) concentration regions in the 2 L bottle displayed 1.5% and 2.0% , respectively. The highest aggregation level of 2.7% was observed in maximum histidine samples (ratio 1.00), whereas minimum histidine samples (ratio 2.58) did not show an increase in HMWS. After 12 months at $-20\text{ }^{\circ}\text{C}$, samples with the initial concentrations contained 2.8% HMWS. Maximum mAb (2.1%), minimum histidine (1.8%), and maximum histidine (2.4%) showed less increase. The highest HMWS levels were found for minimum mAb samples (3.4%).

After 6 months, SVP levels did not increase significantly and remained below 10000 particles per mL in all cases. The buffer control stored at $-20\text{ }^{\circ}\text{C}$ displayed 1700 SVPs per mL after 12 months compared to 900 at t0. Also, after 12 months the total particle count stayed low for the initial concentrations (12700), the minimum mAb (7000), and the minimum histidine samples (9800). In contrast, approximately 230000 SVPs were counted in maximum mAb and 570000 in maximum histidine samples, both containing the highest absolute mAb concentration.

3.3. Long-term storage at $-10\text{ }^{\circ}\text{C}$

Fig. 4 shows that HMWS did not form over 6 weeks storage at $-10\text{ }^{\circ}\text{C}$. After 6 months and 12 months, the HMWS increase for the different formulations was similar to the change at $-20\text{ }^{\circ}\text{C}$, but aggregation was much more pronounced. After 6 months storage, samples with the initial concentrations displayed 3.5% HMWS. The numbers were lower in maximum mAb (2.7%), maximum histidine (2.3%), and minimum histidine (1.6%), but higher in the minimum mAb (4.1%) sample. Similar trends were seen after 12 months. Samples being representative for the initial formulation conditions displayed 4.0% HMWS. Maximum mAb (3.6%), maximum histidine (2.7%), and minimum histidine (1.8%) again contained less soluble aggregates, whereas minimum mAb (5.1%) samples were least stable.

In the histidine buffer control SVP levels increased to $7500\text{ SVPs } \geq 1\text{ }\mu\text{m}$ per mL after 12 months. For all samples, SVPs remained low after 6 weeks storage at $-10\text{ }^{\circ}\text{C}$. In contrast, particle levels were increased in mAb containing samples after 6 months. Samples with the initial concentration showed approximately 450000 SVPs . Minimum mAb and minimum histidine samples displayed only 79300 and 20700 SVPs , respectively. Maximum histidine (207400) and maximum mAb (777200), both containing the highest absolute mAb concentration, led to similar particle levels as the formulation representing the initial mAb concentration. Substantial SVP formation was seen after twelve-month

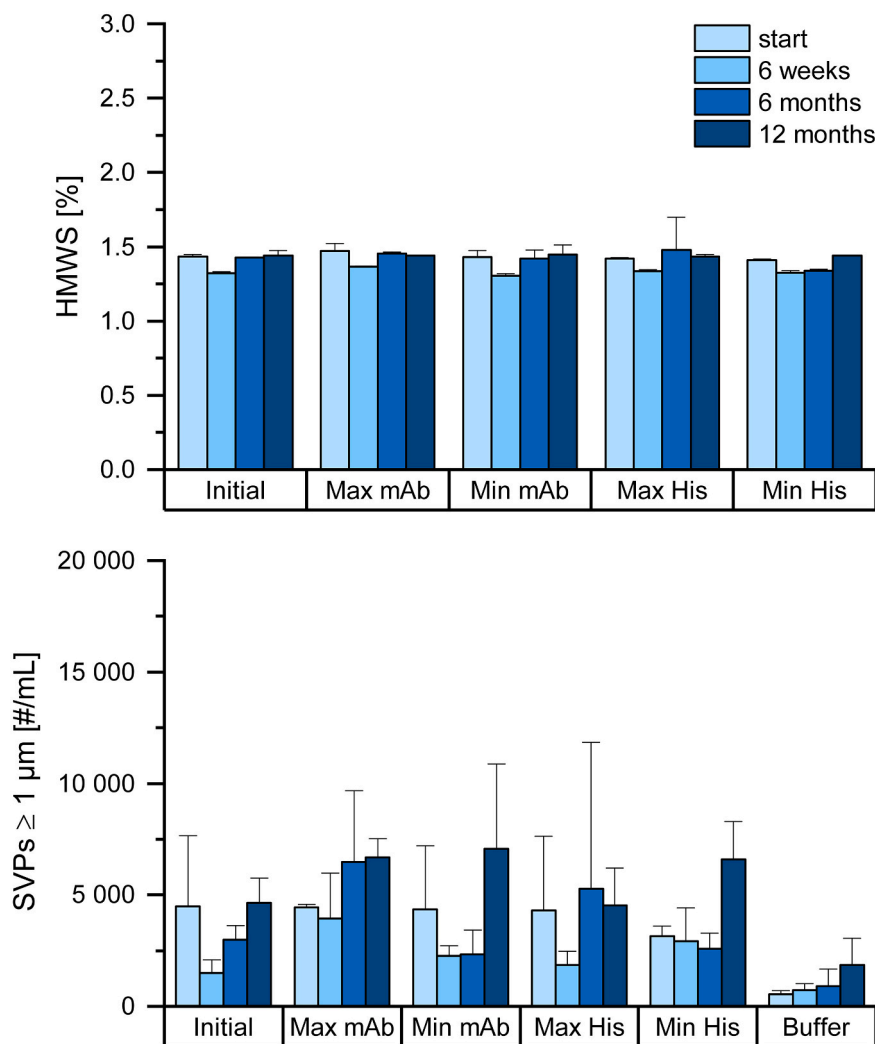


Fig. 2. HMWS and SVPs after storage at $-80\text{ }^{\circ}\text{C}$ up to 12 months.

storage at $-10\text{ }^{\circ}\text{C}$. The trends were the same as after 6 months. In samples representing the initial concentrations 1150800 SVPs $\geq 1 \mu\text{m}$ per mL were detected. Maximum mAb (1316000) and maximum histidine (1092200) gave similar counts. In contrast, samples with minimum mAb and minimum histidine showed tremendously less SVPs $\geq 1 \mu\text{m}$ per mL with only 330100 and 60400, respectively.

3.4. Determination of T_g'

After lyophilisation and subsequent reconstitution with less water, inflection points could automatically be detected by the DSC software in all DSC thermograms (Fig. 5). The highest T_g' ($-30.9\text{ }^{\circ}\text{C}$) was measured for samples containing minimum histidine and consequently the highest mAb to histidine ratio of 2.58. T_g' shifted towards lower temperatures the more the ratio shifted towards histidine. At the initial ratio of 1.61 a T_g' at $-35.3\text{ }^{\circ}\text{C}$ resulted and the maximum mAb (ratio 1.50) sample value was only minimally lower at $-35.6\text{ }^{\circ}\text{C}$. Minimum mAb (ratio 1.16) and maximum histidine (ratio 1.00) samples showed the lowest T_g' values of $-36.3\text{ }^{\circ}\text{C}$ and $-37.1\text{ }^{\circ}\text{C}$, respectively.

4. Discussion

Our aim was to close a gap in knowledge about the stability of biologics, specifically proteins exemplarily studied using a mAb, as frozen bulk material. During industrial production of mAb solutions, bulk drug

substance that is not fully formulated is regularly frozen. Hence, we characterised cryoconcentration after large-scale freezing of a mAb in pure histidine buffer without further excipients (Bluemel et al., 2020). In the recent study, we connected the cryoconcentration, which comes with a change in protein to solute ratio after freezing, to the T_g' and long-term frozen storage stability. At first, we developed a method to analyse the T_g' of pure mAb/histidine mixtures at different concentrations found previously upon freezing in large-scale containers (Fig. 1). The focus was on minimum and maximum mAb and histidine concentrations. DSC thermograms of protein samples that do not contain glass formers such as sugars often do not show a sharp sigmoidal change in heat flow signal (Pansare and Patel, 2016). In such cases, the onset of T_g' can be determined using the first derivative plot. However, this inevitably leads to a deviation between the obtained T_g' and the commonly reported midpoint T_g' (Pansare and Patel, 2016). Therefore, we optimised the sample preparation in order to directly measure the midpoint T_g' , based on the inflection point, of samples that only consist of a mAb and the buffer component. Increasing the sample concentration via lyophilisation and subsequent reconstitution with less water resulted in distinct glass transition signals. This enabled us to determine T_g' as the inflection point. By keeping the mAb to histidine ratio, the T_g' of the solutions was not influenced (Kasper and Friess, 2011; Pansare and Patel, 2016). The T_g' of a solution depends on the sample composition, but is independent of the initial concentration (Franks, 1998; Kasper and Friess, 2011). Additionally, higher histidine concentrations than expected from its

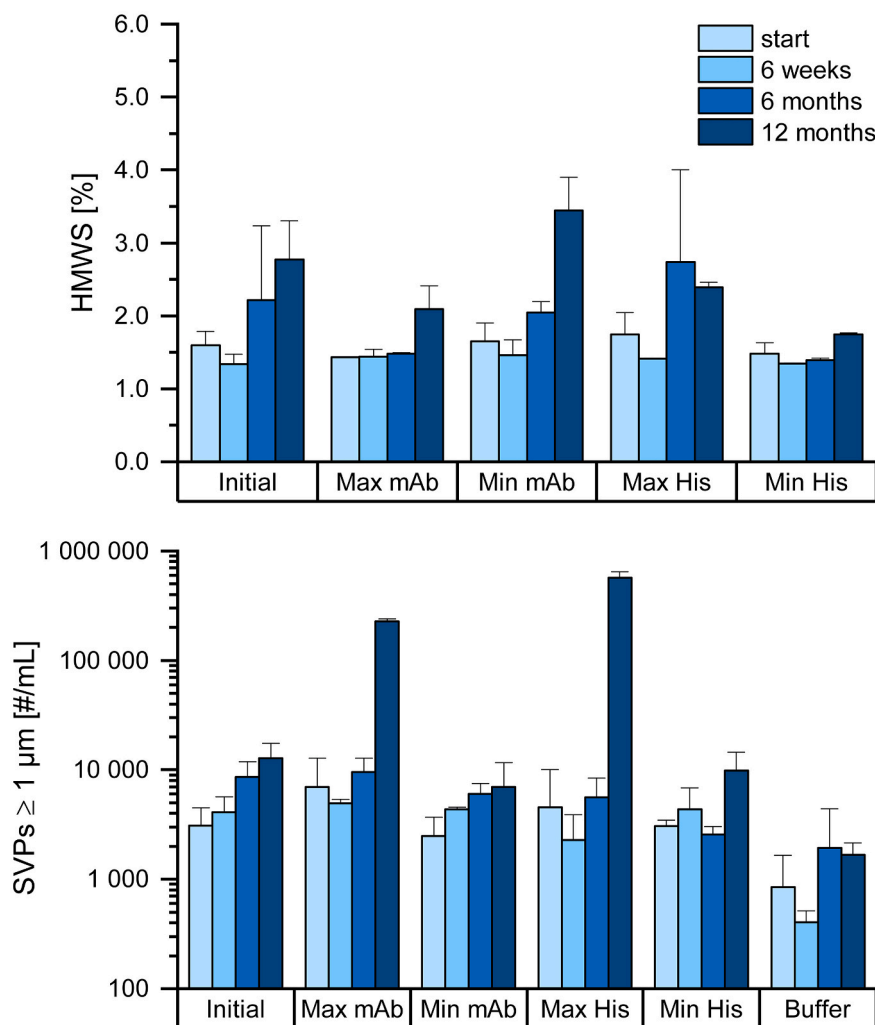


Fig. 3. HMWS and SVPs after storage at $-20\text{ }^{\circ}\text{C}$ up to 12 months.

solubility product could be reached via this method. Histidine is known to form an amorphous phase upon freezing of aqueous solutions and to keep its glassy state throughout lyophilisation (Österberg and Wadsten, 1999). In combination with the high mAb concentration, which is preventing buffer crystallisation (Thorat et al., 2020), this may support to reach such high histidine concentrations by lyophilisation and reconstitution with less volume (Włodarski et al., 2014). By reducing the heating rate to 3 K/min we could avoid an interference of the ice melting endotherm with the glass transition endotherm. The samples significantly differed in T_g' between approximately $-31\text{ }^{\circ}\text{C}$ (minimum histidine) for the highest and $-37\text{ }^{\circ}\text{C}$ (maximum histidine) for the lowest mAb to histidine ratio. In comparison, the pure mAb shows a T_g' of $-18\text{ }^{\circ}\text{C}$. It has been shown that higher salt concentrations lower the overall T_g' of the formulation matrix (Kuelzto et al., 2008; Pansare and Patel, 2016).

None of the samples showed aggregate formation when stored well below T_g' at $-80\text{ }^{\circ}\text{C}$. After storage at $-20\text{ }^{\circ}\text{C}$, both HMWS and SVPs levels were increased. This effect, already discernible after 6 months, was boosted after 12 months. Similar trends, but even more pronounced, were detected at $-10\text{ }^{\circ}\text{C}$. Relative aggregation, assessed via SEC, was highest in samples with the lowest mAb concentration. Maximum mAb but also maximum histidine samples displayed considerably lower HMWS levels. In contrast, when focusing on the absolute aggregation level assessed via SVPs, increasing mAb concentration negatively affected colloidal stability. At $-20\text{ }^{\circ}\text{C}$, maximum mAb and maximum histidine samples in particular formed insoluble aggregates. At $-10\text{ }^{\circ}\text{C}$,

SVPs counts were still highest for samples with the highest absolute mAb concentration (maximum mAb and maximum histidine), but also in mAb samples representing the initial composition significant SVP formation occurred. At the lowest absolute mAb concentration significantly less SVPs were found. It appears that the mAb concentration affects the stability, however the mAb to histidine ratio was not kept constant. The change in mAb concentration comes with a shift of the mAb to excipient ratio and consequently of T_g' as well as ionic strength in the FCM. This might explain why minimum histidine samples with a moderate mAb concentration showed highest stability in all cases.

The solution T_g' is a key parameter for frozen storage stability (Alhalaweh et al., 2015; Kolhe et al., 2009). Below T_g' , the unfrozen FCM forms a glassy state, a solid solution of cryoconcentrated solutes and unfrozen, amorphous water (Lim et al., 2006). The viscosity of this glass is in the order of 10^{14} Pas, so that motion is in the range of mm/year (Kasper and Friess, 2011; Pansare and Patel, 2016). Ultimately, molecular mobility is greatly reduced and mAb aggregation prevented (Miller et al., 2013). Consequently, neither soluble nor insoluble aggregates were detected, when samples were stored at $-80\text{ }^{\circ}\text{C}$, more than $40\text{ }^{\circ}\text{C}$ below T_g' . It has been shown for lyophilisates that storage at temperatures slightly below the glass transition T_g does not necessarily result in complete prevention of aggregation (Chang et al., 1996). Assuming that these findings can be transferred to T_g' , we propose that a safety margin should be considered when choosing the appropriate storage temperature for frozen protein solutions. Alhalaweh et al. highlighted that ΔT of $20\text{ }^{\circ}\text{C}$ between T_g and storage temperature of lyophilisates is sufficient to

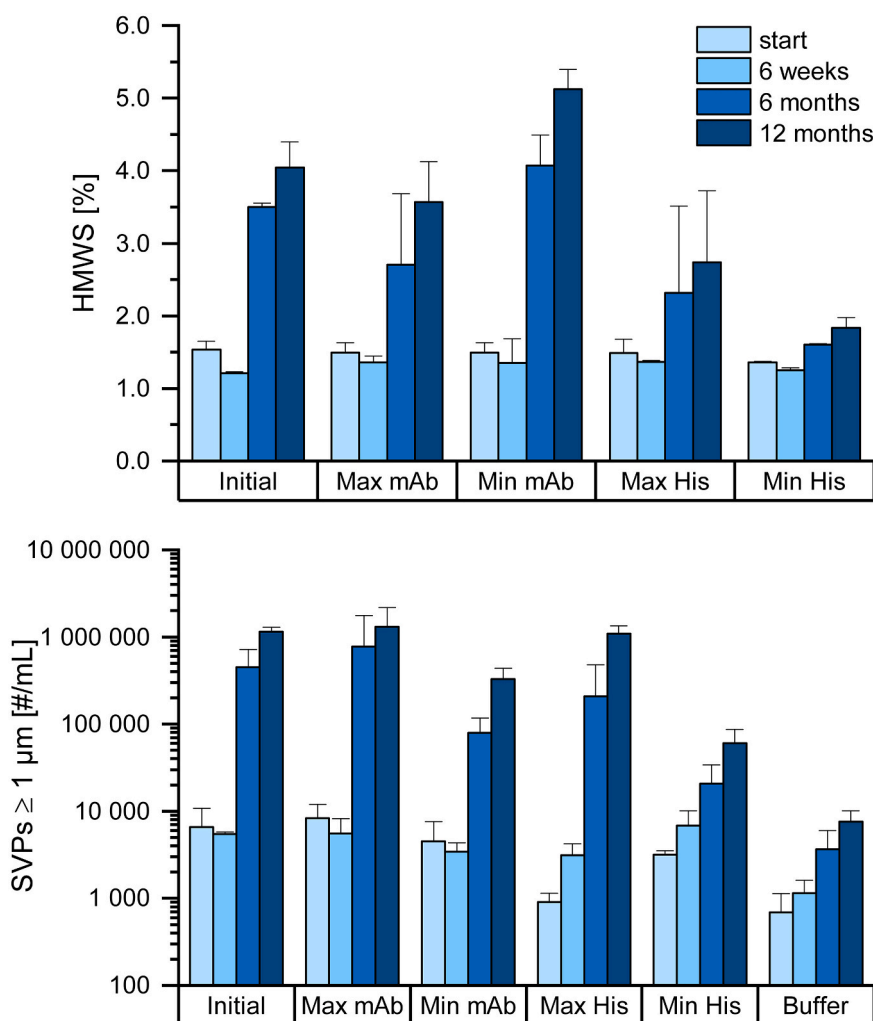


Fig. 4. HMWS and SVPs after storage at $-10\text{ }^{\circ}\text{C}$ up to 12 months.

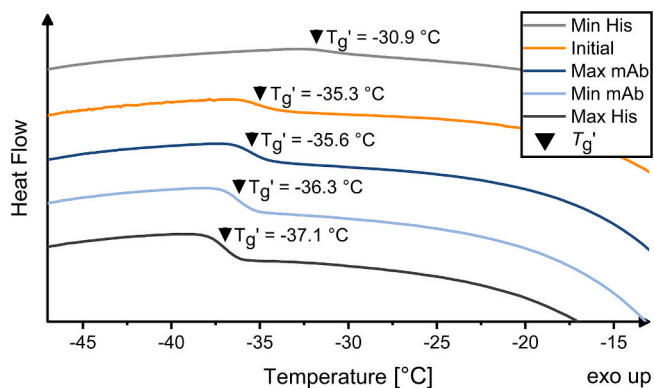


Fig. 5. DSC thermograms of samples with different mAb to histidine ratios. The ratio of the samples was: Min His (2.58), Initial (1.61), Max mAb (1.50), Min mAb (1.16), Max His (1.00).

essentially reduce mobility to a level that aggregation becomes minimal (Alhalaweh et al., 2015). In contrast, when samples are stored above T_g' , the viscosity drops, facilitating irreversible denaturation and aggregation (Franks, 1998). Above T_g' , the viscosity of the FCM decreases exponentially with increasing temperature (Seifert and Friess, 2020). The lower viscosity is associated with increased molecular mobility and consequently accelerated physical and chemical instability (Pansare and

Patel, 2016). Correspondingly, we saw marked mAb aggregation upon storage at temperatures above T_g' , which was much more pronounced at $-10\text{ }^{\circ}\text{C}$ compared to $-20\text{ }^{\circ}\text{C}$. Nevertheless, it took several months until the stability was markedly impacted. Lim et al. investigated the influence of glass transition and storage temperature of frozen peas on quality attributes (Lim et al., 2006). They found that the loss of quality is relative to ΔT between T_g' and storage temperature. Transferring these findings to the mAb samples, reflecting different regions within a frozen large bottle, the sample stability would decrease according to their T_g' , which is defined by their mAb to histidine ratio (Fig. 5): minimum histidine \gg initial $>$ maximum mAb $>$ minimum mAb $>$ maximum histidine. This can explain why samples containing minimum histidine showed the highest stability during storage above T_g' , whereas maximum histidine displayed significantly less colloidal stability at both temperatures. These differences in T_g' , driven by the composition of the FCM but not by the initial concentration (Authelin et al., 2020; Connolly et al., 2015; Franks, 1998; Kasper and Friess, 2011), clearly affected stability.

In addition, not only T_g' but also the ionic strength in the FCM is impacted by the mAb to histidine ratio. The ionic strength of a solution affects mAb aggregation (Wang et al., 2010). Though the net effect of ionic strength on aggregation is dependent on the specific mAb, its protein-protein interactions, and the salt type, the ionic strength is undeniably a key parameter. Ions interact electrostatically with mAbs and thereby influence protein-protein interactions and the conformational state. In addition, electrostatic interactions between the FCM and the ice

surface were hypothesized (Arsiccio and Pisano, 2020). In the recent study, lower ionic strength in the non-solidified FCM increased stability. Most likely protein-protein interactions and electrostatic interactions with the ice surface were enhanced by higher salt concentrations. Not necessarily all results can be explained by T_g' and ionic strength effects alone. While the colloidal stability for samples with the lowest mAb to histidine ratio was reduced, the formation of soluble aggregates was decreased. Maximum mAb samples displayed equivalent low HMWS levels. Both samples contain the highest absolute mAb concentration. In contrast, minimum mAb concentration led to the highest relative HMWS fraction. Several studies highlighted that surface-induced local enrichment and denaturation play an important role in mAb aggregation (Duarte et al., 2020; Sarciaux et al., 1999; Singh et al., 2009). Possible mechanisms of ice-induced denaturation at the interface are discussed, such as adsorption, pH shifts, accumulation of air bubbles, increased pressure, and enhanced cold denaturation (Arsiccio and Pisano, 2020). To reduce dissimilarity in ice morphology in the samples, we used controlled nucleation during sample preparation (Bhatnagar et al., 2008; Kasper and Friess, 2011). Thereby, we aimed to focus on the influence of the sample composition on storage stability and eliminate any interface related influence. But Ostwald ripening may occur upon storage at $-20\text{ }^\circ\text{C}$ as well as $-10\text{ }^\circ\text{C}$. It has been highlighted before, that the number of protein molecules that adsorb to the interface is limited by the total interface area. (Arsiccio and Pisano, 2020; Wang, 2000). Consequently, the relative adsorbed fraction decreases with increasing absolute mAb concentration (Arsiccio and Pisano, 2020; Jiang and Nail, 1998). Our results suggest that the formation of HMWS is also driven by the enrichment of protein molecules and their aggregation at the FCM/ice interface. In respect of SVPs, levels remained low in the histidine buffer control. A miniscule increase upon storage at $-10\text{ }^\circ\text{C}$ up to 12 months might be due to the laboratory environment and potential oxidation processes (Mason et al., 2010). For mAb containing samples, increasing absolute mAb concentration had a negative impact on the formation of insoluble aggregates. While surface-induced denaturation is limited, the SVPs levels, which are not measured relatively, increased with mAb concentration. The formation of SVPs detected via flow imaging microscopy might result from hundredth of a percent of the total protein in solution (Barnard et al., 2011). Thus, samples that showed low relative aggregation because of their high mAb concentration, displayed highest absolute SVPs levels. Protein-protein interactions in the unfrozen FCM might facilitate the formation of SVPs at higher mAb concentration. It should be noted that insoluble particles are not covered by SEC measurement and flow imaging microscopy via Flowcam® detects insoluble particles $\geq 1\text{ }\mu\text{m}$. Insoluble aggregates in the nanometre range were not tracked by these methods. Dynamic light scattering measurements could have closed that gap and should be considered for future studies that examine long-term frozen storage stability of proteins as a qualitative method.

When these small-scale results are transferred to the cryoconcentration that we found in a 2 L bottle after large-scale freezing (Bluemel et al., 2020), marked differences in stability can be associated with the apparently small changes in concentration. The highly concentrated top region of the bottle with maximum mAb concentration and the highly concentrated area with maximum histidine tend to form less HMWS compared to samples with the initial concentration, but significantly contribute to the formation of SVPs. In contrast, the diluted core of the bottle with minimum mAb can be associated with moderate SVPs formation but increased HMWS. The minimum histidine region at the bottle wall is characterised by highest stability.

Thus, the study highlights that a shift in the ratio of protein to small excipient molecules in different regions of large-scale frozen containers of bulk drug substance can substantially impact the quality of the product. Storage at $-80\text{ }^\circ\text{C}$ can level off the effect. We studied the effect over one-year storage at temperatures $10\text{ }^\circ\text{C}$ to $20\text{ }^\circ\text{C}$ above T_g' to enhance the effect. Frequently drug substance is stored for much longer times. Future studies have to focus on temperatures slightly below T_g' as

it would be an enormous contribution to sustainability if storage of frozen drug substance would not require $-80\text{ }^\circ\text{C}$ but e.g. $-40\text{ }^\circ\text{C}$ would be sufficiently low.

Overall, many other effects have to be considered before generalising the conclusion of our study. The regions in a large-scale freezing container significantly differ in freezing time and therefore ice morphology which could affect local mAb stability. Furthermore, local pressure or air bubbles and consequently oxidation could be affected by the position. Cryoconcentration can be reduced by faster freezing rates, which would additionally reduce the exposure time of the protein to a non-solidified FCM above T_g' (Singh et al., 2009), but would also result in smaller ice crystals and consequently larger interfaces. Another way to reduce cryoconcentration is directed freezing from bottom to top. Thereby, natural convection, the main driving force for cryoconcentration, can be prevented (Rodrigues et al., 2013). In addition, optimisation of the formulation can decrease the risk of aggregation. In that respect, we highlight in our study that the interplay of the mAb to histidine ratio, determining T_g' and the ionic strength in the FCM, and the absolute mAb concentration has to be considered. ΔT between T_g' and the storage temperature can be optimised by avoiding excipients forming cryoconcentrates with low T_g' . The ionic strength can be reduced by using minimal salt and buffer concentrations. By increasing the initial mAb concentration, the relative fractions that aggregate upon long-term frozen storage can be decreased.

5. Conclusion

In a previous study, we characterised the cryoconcentration in a 2 L bottle after large-scale freezing of mAb in pure histidine buffer (Bluemel et al., 2020). We found significant changes in mAb concentration that were associated with shifts in mAb to histidine ratio. In this work, we characterised long-term frozen storage stability of respective samples with focus on mAb aggregation.

We analysed the T_g' of samples, which do not contain a glass forming sugar and which reflect the different regions in the bottle, via an optimised DSC method. Samples were lyophilised and subsequently reconstituted in less volume to increase signal strength in DSC thermograms. T_g' of samples ranged between $-31\text{ }^\circ\text{C}$ and $-37\text{ }^\circ\text{C}$ and was defined by the mAb to histidine ratio. mAb stability was not affected when samples were stored below T_g' at $-80\text{ }^\circ\text{C}$. Long-term mAb stability upon storage above T_g' , at $-20\text{ }^\circ\text{C}$ or $-10\text{ }^\circ\text{C}$, was found to be an interplay of T_g' , the ionic strength in the non-solidified FCM, and the mAb concentration. ΔT between T_g' and the storage temperature had a marked impact on stability. Consequently, stability was higher at $-20\text{ }^\circ\text{C}$ than at $-10\text{ }^\circ\text{C}$. Samples with the highest mAb to histidine ratio and thus highest T_g' and lowest ionic strength in the FCM displayed least formation of soluble and insoluble aggregates. In addition, the absolute mAb concentration affected storage stability. The relative aggregated fraction, assessed via SEC, decreased with increasing mAb concentration. In contrast, absolute aggregation in respect of SVPs was negatively affected, pointing to an additional protein-protein interaction effect.

Transferred to cryoconcentration in a 2 L bottle, apparently small changes in mAb and excipient concentration and shifts in mAb to histidine ratio have a marked impact on long-term frozen storage stability. Regions with increased mAb concentration, in case of a 2 L bottle the centre near the bottom and the top region, tend to form SVPs, while a lower mAb concentration, in case of a 2 L bottle in the core, leads to enhanced formation of HMWS. The highest stability can be expected for the areas with lowest histidine concentration at the wall.

Further studies will focus on possible correlations between mAb and buffer concentration that are systematically varied and long-term stability during frozen storage. In addition, storage at intermediate temperatures below T_g' , e.g. $-40\text{ }^\circ\text{C}$, could contribute to the sustainability of long-term frozen storage, but requires detailed studies of the cryoconcentration effects and formulation impacts. Frozen storage stability will be impacted if a cryoprotectant is added which increases viscosity

and provides spacing between mAb molecules in the freeze concentrate decreasing mAb aggregation.

Declaration of Competing Interest

The authors declare that they have no known competing financial interests or personal relationships that could have appeared to influence the work reported in this paper.

Acknowledgements

The authors thank the Novartis Pharma AG for providing mAb stock solutions.

References

- Alhalaweh, A., Alzghoul, A., Mahlin, D., Bergström, C.A.S., 2015. Physical stability of drugs after storage above and below the glass transition temperature: Relationship to glass-forming ability. *Int. J. Pharmaceut.* 495, 312–317. <https://doi.org/10.1016/j.ijpharm.2015.08.101>.
- Arsiccio, A., Pisano, R., 2020. The ice-water interface and protein stability: a review. *J. Pharm. Sci.* 109, 2116–2130. <https://doi.org/10.1016/j.xphs.2020.03.022>.
- Arsiccio, A., McCarty, J., Pisano, R., Shea, J.-E., 2020. Heightened cold-denaturation of proteins at the ice–water interface. *J. Am. Chem. Soc.* 142, 5722–5730. <https://doi.org/10.1021/jacs.9b13454>.
- Authelin, J.-R., Rodrigues, M.A., Tchessalov, S., Singh, S.K., McCoy, T., Wang, S., Shalaev, E., 2020. Freezing of biologicals revisited: scale, stability, excipients, and degradation stresses. *J. Pharm. Sci.* 109, 44–61. <https://doi.org/10.1016/j.xphs.2019.10.062>.
- Barnard, J.G., Singh, S., Randolph, T.W., Carpenter, J.F., 2011. Subvisible particle counting provides a sensitive method of detecting and quantifying aggregation of monoclonal antibody caused by freeze-thawing: insights into the roles of particles in the protein aggregation pathway. *J. Pharm. Sci.* 100, 492–503. <https://doi.org/10.1002/jps.22305>.
- Bhatnagar, B.S., Pikal, M.J., Bogner, R.H., 2008. Study of the individual contributions of ice formation and freeze-concentration on isothermal stability of lactate dehydrogenase during freezing. *J. Pharm. Sci.* 97, 798–814. <https://doi.org/10.1002/jps.21017>.
- Bluemel, O., Buecheler, J.W., Rodrigues, M.A., Geraldes, V., Hoelzl, G., Bechtold-Peters, K., Friess, W., 2020. Cryoconcentration and 3D temperature profiles during freezing of mAb solutions in large-scale pet bottles and a novel scale-down device. *Pharm. Res.* 37, 179. <https://doi.org/10.1007/s11095-020-02886-w>.
- Chang, B.S., Beauvais, R.M., Dong, A., Carpenter, J.F., 1996. Physical factors affecting the storage stability of freeze-dried interleukin-1 receptor antagonist: glass transition and protein conformation. *Arch. Biochem. Biophys.* 331, 249–258. <https://doi.org/10.1006/abbi.1996.0305>.
- Connolly, B.D., Le, L., Patapoff, T.W., Cromwell, M.E.M., Moore, J.M.R., Lam, P., 2015. Protein aggregation in frozen trehalose formulations: effects of composition, cooling rate, and storage temperature. *J. Pharm. Sci.* 104, 4170–4184. <https://doi.org/10.1002/jps.24646>.
- Duarte, A., Rego, P., Ferreira, A., Dias, P., Geraldes, V., Rodrigues, M.A., 2020. Interfacial stress and container failure during freezing of bulk protein solutions can be prevented by local heating. *AAPS PharmSciTech* 21, 251. <https://doi.org/10.1208/s12249-020-01794-x>.
- Franks, F., 1998. Freeze-drying of bioproducts: putting principles into practice. *Eur. J. Pharm. Biopharm.* 45, 221–229. [https://doi.org/10.1016/S0939-6411\(98\)00004-6](https://doi.org/10.1016/S0939-6411(98)00004-6).
- Hauptmann, A., Podgoršek, K., Kuzman, D., Srčić, S., Hoelzl, G., Loerting, T., 2018. Impact of buffer, protein concentration and sucrose addition on the aggregation and particle formation during freezing and thawing. *Pharm. Res.* 35, 101. <https://doi.org/10.1007/s11095-018-2378-5>.
- Hauptmann, A., Hoelzl, G., Loerting, T., 2019. Distribution of protein content and number of aggregates in monoclonal antibody formulation after large-scale freezing. *AAPS PharmSciTech* 20, 72. <https://doi.org/10.1208/s12249-018-1281-z>.
- Jiang, S., Nail, S.L., 1998. Effect of process conditions on recovery of protein activity after freezing and freeze-drying. *Eur. J. Pharm. Biopharm.* 45, 249–257. [https://doi.org/10.1016/S0939-6411\(98\)00007-1](https://doi.org/10.1016/S0939-6411(98)00007-1).
- Kasper, J.C., Friess, W., 2011. The freezing step in lyophilization: Physico-chemical fundamentals, freezing methods and consequences on process performance and quality attributes of biopharmaceuticals. *Eur. J. Pharm. Biopharm.* 78, 248–263. <https://doi.org/10.1016/j.ejpb.2011.03.010>.
- Kolhe, P., Amend, E., Singh, K., 2009. Impact of freezing on pH of buffered solutions and consequences for monoclonal antibody aggregation. *Biotechnol. Prog.* 26, 727–733. <https://doi.org/10.1002/btpr.377>.
- Kolhe, P., Mehta, A.P., Lary, A.L., Chico, S.C., Singh, S.K., 2012. Large-Scale Freezing of Biologics (Part III). *BioPharm Int.* 25, 40–48.
- Kueltzo, L.A., Wang, W.E.L., Randolph, T.W., Carpenter, J.F., 2008. Effects of solution conditions, processing parameters, and container materials on aggregation of a monoclonal antibody during freeze-thawing. *J. Pharm. Sci.* 97, 1801–1812. <https://doi.org/10.1002/jps.21110>.
- Lim, M., Wu, H., Breckell, M., Birch, J., 2006. Influence of the glass transition and storage temperature of frozen peas on the loss of quality attributes. *Int. J. Food Sci. Technol.* 41, 507–512. <https://doi.org/10.1111/j.1365-2621.2005.01096.x>.
- Mason, B.D., McCracken, M., Bures, E.J., Kerwin, B.A., 2010. Oxidation of Free L-histidine by tert-Butylhydroperoxide. *Pharm. Res.* 27, 447–456. <https://doi.org/10.1007/s11095-009-0032-y>.
- Mehta, S.B., Subramanian, S., D'Mello, R., Brisbane, C., Roy, S., 2019. Effect of protein cryoconcentration and processing conditions on kinetics of dimer formation for a monoclonal antibody: a case study on bioprocessing. *Biotechnol. Prog.* 35, 1–7. <https://doi.org/10.1002/btpr.2836>.
- Miller, M.A., Rodrigues, M.A., Glass, M.A., Singh, S.K., Johnston, K.P., Maynard, J.A., 2013. Frozen-state storage stability of a monoclonal antibody: aggregation is impacted by freezing rate and solute distribution. *J. Pharm. Sci.* 102, 1194–1208. <https://doi.org/10.1002/jps.23473>.
- Österberg, T., Wadsten, T., 1999. Physical state of l-histidine after freeze-drying and long-term storage. *Eur. J. Pharm. Sci.* 8, 301–308. [https://doi.org/10.1016/S0928-0987\(99\)00028-7](https://doi.org/10.1016/S0928-0987(99)00028-7).
- Padala, C., Jameel, F., Rathore, N., Gupta, K., Sethuraman, A., 2010. Impact of uncontrolled vs controlled rate freeze-thaw technologies on process performance and product quality. *PDA J. Pharm. Sci. Technol.* 64, 290–298.
- Pansare, S.K., Patel, S.M., 2016. Practical considerations for determination of glass transition temperature of a maximally freeze concentrated solution. *AAPS PharmSciTech* 17, 805–819. <https://doi.org/10.1208/s12249-016-0551-x>.
- Rathore, N., Rajan, R.S., 2008. Current perspectives on stability of protein drug products during formulation, fill and finish operations. *Biotechnol. Prog.* 24, 504–514. <https://doi.org/10.1021/bp070462h>.
- Rodrigues, M.A., Miller, M.A., Glass, M.A., Singh, S.K., Johnston, K.P., 2011. Effect of freezing rate and dendritic ice formation on concentration profiles of proteins frozen in cylindrical vessels. *J. Pharm. Sci.* 100, 1316–1329. <https://doi.org/10.1002/jps.22383>.
- Rodrigues, M.A., Balzan, G., Rosa, M., Gomes, D., de Azevedo, E.G., Singh, S.K., Matos, H.A., Geraldes, V., 2013. The importance of heat flow direction for reproducible and homogeneous freezing of bulk protein solutions. *Biotechnol. Prog.* 29, 1212–1221. <https://doi.org/10.1002/btpr.1771>.
- Roessl, U., Jajcevic, D., Leitgeb, S., Khinast, J.G., Nidetzky, B., 2014. Characterization of a laboratory-scale container for freezing protein solutions with detailed evaluation of a freezing process simulation. *J. Pharm. Sci.* 103, 417–426. <https://doi.org/10.1002/jps.23814>.
- Roessl, U., Leitgeb, S., Nidetzky, B., 2015. Protein freeze concentration and micro-segregation analysed in a temperature-controlled freeze container. *Biotechnol. Rep.* 6, 108–111. <https://doi.org/10.1016/j.btre.2015.03.004>.
- Sarciaux, J.-M., Mansour, S., Hageman, M.J., Nail, S.L., 1999. Effects of buffer composition and processing conditions on aggregation of bovine IgG during freeze-drying. *J. Pharm. Sci.* 88, 1354–1361. <https://doi.org/10.1021/js980383n>.
- Seifert, I., Friess, W., 2020. Freeze concentration during freezing: how does the maximally freeze concentrated solution influence protein stability? *Int. J. Pharmaceut.* 589, 119810. <https://doi.org/10.1016/j.ijpharm.2020.119810>.
- Singh, S.K., Kolhe, P., Wang, W., Nema, S., 2009. Large-scale freezing of biologics a practitioner's review, part one: fundamental aspects. *Bioprocess Int.* 7, 32–44.
- Singh, S.K., Kolhe, P., Mehta, A.P., Chico, S.C., Lary, A.L., Huang, M., 2011. Frozen state storage instability of a monoclonal antibody: aggregation as a consequence of trehalose crystallization and protein unfolding. *Pharm. Res.* 28, 873–885. <https://doi.org/10.1007/s11095-010-0343-z>.
- Thorat, A.A., Munjal, B., Geders, T.W., Suryanarayanan, R., 2020. Freezing-induced protein aggregation - Role of pH shift and potential mitigation strategies. *J. Control. Release* 323, 591–599. <https://doi.org/10.1016/j.jconrel.2020.04.033>.
- Wang, W., 2000. Lyophilization and development of solid protein pharmaceuticals. *Int. J. Pharmaceut.* 203, 1–60. [https://doi.org/10.1016/S0378-5173\(00\)00423-3](https://doi.org/10.1016/S0378-5173(00)00423-3).
- Wang, W., Nema, S., Teagarden, D., 2010. Protein aggregation—Pathways and influencing factors. *Int. J. Pharmaceut.* 390, 89–99. <https://doi.org/10.1016/j.ijpharm.2010.02.025>.
- Włodarski, K., Sawicki, W., Paluch, K.J., Tajber, L., Grembecka, M., Hawelek, L., Wojnarowska, Z., Grzybowska, K., Talik, E., Paluch, M., 2014. The influence of amorphization methods on the apparent solubility and dissolution rate of tadalafil. *Eur. J. Pharm. Sci.* 62, 132–140. <https://doi.org/10.1016/j.ejps.2014.05.026>.
- Zhang, A., Singh, S.K., Shirts, M.R., Kumar, S., Fernandez, E.J., 2012. Distinct aggregation mechanisms of monoclonal antibody under thermal and freeze-thaw stresses revealed by hydrogen exchange. *Pharm. Res.* 29, 236–250. <https://doi.org/10.1007/s11095-011-0538-y>.